

Effect of the Physicochemical Properties on the Permeation Performance in Fully Aromatic Crosslinked Polyamide Thin Films

Il Juhn Roh

Department of Mechanical Engineering, University of Colorado at Boulder, Boulder, Colorado 80309-0427

Received 24 January 2002; accepted 7 May 2002

ABSTRACT: Thin-film-composite reverse-osmosis (RO) membranes were prepared by the interfacial polymerization of trifunctional 1,3,5-benzotricarbonyl chloride (TMC) with difunctional 1,3-benzendiamine (MPDA) or 1,4-benzendiamine (PPDA). The meta-positioned polyamide (MPDA/TMC) resulted in higher water flux but lower salt rejection than the para-positioned polyamide (PPDA/TMC). To understand this behavior, we studied various factors including the thickness, rupture strength, chemical properties, and solubilities of the water and salt in the thin-film polyamide. The thin films made from MPDA and PPDA possessed similar thicknesses and rupture strengths adequate for with-

standing the RO operation pressure. However, the meta-positioned polyamide had higher hydrophilicity and greater molecular chain mobility than the para-positioned polyamide, resulting in higher water flux. In contrast, the para-positioned polyamide had lower salt solubility and lower molecular chain mobility than the meta-positioned polyamide, thereby possessing higher salt rejection. © 2002 Wiley Periodicals, Inc. *J Appl Polym Sci* 87: 569–576, 2003

Key words: membranes; thin films; polyamides; structure-property relations; selectivity

INTRODUCTION

High permeability and selectivity are desirable properties for reverse-osmosis (RO) membranes. For a membrane to possess these properties, the active layer of the membrane should be very thin and hydrophilic in nature. Thin-film-composite (TFC) membranes meet this demand. The active layer of a TFC is a thin film that controls the passage of the solvent (water) and solutes. Aromatic network polyamide thin films fabricated via interfacial polymerization (IP) have proven to be the most successful permselective layers.^{1–4}

An understanding of the solvent and solute transport mechanisms through the active layer is of foremost importance for enhancing permeation performance. To this end, there have been many modeling approaches to and much research on the thin-film active layer,^{5,6} and numerous researchers have experimented with a variety of membrane formation schemes and polymers to obtain a thin, high-permeability active layer.^{7–11} However, the active layers of most commercially successful TFC membranes are extremely thin and have a crosslinked structure. Consequently, they are insoluble in common solvents, bringing about sampling problems for characterization with

conventional analytical techniques. Therefore, many researchers have sought to optimize the active-layer performance by experimenting with a variety of membrane formation schemes and polymers and inferring the interrelation between the permeation performance and the chemical structure of the monomers.^{12–14} In contrast, the characterization of the active layer to elucidate the effect of the intrinsic polymer material properties of the active layer together with the physicochemical properties and mechanical properties on the permeation properties is rarely found in the literature.^{15–17} Therefore, the characterization of the active layer for an understanding of the effect of the inherent material properties on the permeation characteristics should be established.

In this research, we have tried to characterize the inherent polymer material physicochemical properties to elucidate the factors affecting the permeation. Two crosslinked, fully aromatic polyamides were synthesized via the IP of two different phenylene diamines with trifunctional acyl chloride. The interrelationships between their permeation characteristics and the intrinsic polymer properties, including the mechanical strength, thickness, solubility of the solvent and solute, and mobility of the molecular chain, are considered.

TRANSPORT MECHANISM

To study the transport properties through a thin active layer, I briefly introduce the transport mechanism for

Correspondence to: I. J. Roh (rohi@colorado.edu).

RO membranes. Although a number of mechanisms have been proposed, the solution-diffusion transport mechanism proposed by Lonsdale et al.⁵ is one of the most widely accepted transport mechanisms. Therefore, I adopted this transport mechanism to explain the transport properties of these membranes. According to this mechanism, both the solvent and solute molecules are dissolved in the nonporous active layer of the membrane and are subsequently transported by diffusion in an uncoupled manner. The water flux (J_w) is given by

$$J_w = \frac{D_w C_w \bar{V}_w}{R_g T d} (\Delta P - \Delta \Pi) \quad (1)$$

$$J_s = \frac{D_s K_s}{d} \Delta C_s \quad (2)$$

where J_s is the salt flux; D_w and D_s are the diffusion coefficients of water and salt in the membrane, respectively; C_w and K_s are the concentration of dissolved water in the membrane and the partition coefficient of salt between the membrane and solution, respectively; and $C_w D_w$ and $K_s D_s$ represent the water and salt permeability coefficients, respectively. \bar{V}_w is the partial molar volume of water in the external phase. $\Delta P = P' - P''$ and $\Delta \Pi = \Pi' - \Pi''$ are the applied pressure difference and osmotic pressure difference across the membrane, respectively. $\Delta C_s = C_s' - C_s''$ is the concentration difference of salt in the two sides of the membrane. The prime and double-prime superscripts refer to the feed and the permeation sides, respectively. R_g is the gas constant, T is the absolute temperature, and d is the active-layer thickness. The important material properties of the active layer that affect permeation through the membrane are the equilibrium solubilities (C_w and K_s) and the solute and solvent diffusivities (D_w and D_s). It is the combined effect of these two properties that determines the permeability and selectivity of the membrane.

EXPERIMENTAL

Materials

For the interfacial synthesis of the active-layer polymers, diamines and triacyl chloride were used. The triacyl chloride used in this study was 1,3,5-benzenetricarbonyl chloride (TMC; Aldrich, Milwaukee, WI, 98%). Before being used for thin-film synthesis, TMC was distilled in vacuum at 160°C. The purified TMC was stored in a vacuum desiccator containing calcium chloride to prevent hydrolysis of the acyl chloride groups. The diamines included 1,3-benzendiamine (MPDA; Aldrich; 99%) and 1,4-benzendiamine (PPDA; Aldrich; 99%). MPDA was distilled in vacuum

at 170°C, and PPDA was sublimated in vacuum at 50°C. The purified diamines were filled in a dark bottle with N₂ gas and stored in a refrigerator.

The solvent for TMC, *n*-hexane, was dried via shaking with magnesium sulfate and distillation. Before the purified *n*-hexane was used (within 1–2 days), it was stored in a tightly closed bottle with Molecular Sieve A® to prevent the dissolution of water. For the preparation of the diamine solution, RO-purified and deionized water was used.

Polymer preparation

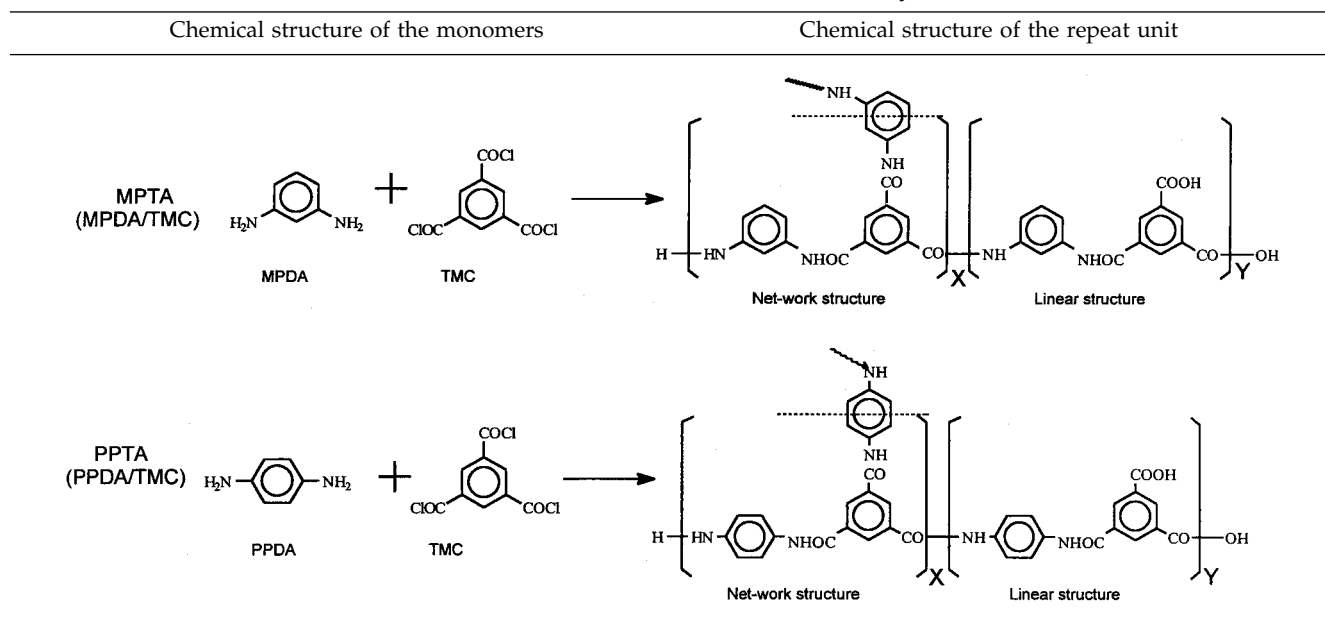
The two crosslinked aromatic polyamides were synthesized via the IP of a 0.5% (w/v) aqueous diamine solution with MPDA or PPDA and a 0.1% (w/v) *n*-hexane acyl chloride (TMC) solution without any support layer. The IP was conducted with an unstirred nondispersion method for 2 min at 20°C. The thin films formed at the interface of the two solutions were retrieved and washed with acidic water, fresh water, and finally methanol to remove the unreacted monomer remnants and occluded salt. The pure solid polymers were dried in vacuum at room temperature and then used with no further post treatment. These polymers were used for the measurement of water and salt solubilities. The chemical structures of these polyamides are believed to be as shown in Table I.

Permeability tests

For the measurement of membrane permeability, TFC membranes were fabricated. The active-layer polymers were synthesized under reaction conditions identical to those for the polymer sample preparation (described previously). However, in this case, the active layer was synthesized over a support layer. The TFC membranes were prepared via a two-step process: first, an asymmetric support polysulfone membrane was fabricated, and then the thin-film active layer was synthesized on its surface. The asymmetric support layers were made as described elsewhere.¹⁴ The thin-film active layers were prepared by in situ IP on the support layer with an unstirred nondispersion method described in an earlier article.¹⁷ The concentrations of the diamines and acyl chloride were fixed at 0.5 and 0.1% (w/v), respectively. The fabricated TFC membranes were washed with acidic water and fresh water to remove the unreacted monomer remnants and occluded salt and then were used for permeation testing with no further post treatment.

The water and salt permeation values were measured with continuous high-pressure RO testing equipment (BSO-100K-3, Akico Co., Japan). A diaphragm pump was used for recycling the aqueous salt solution (NaCl, 2000 ppm) through the system at 3.03 MPa. The temperature of the feed tank, with a 30-L

TABLE I
Chemical Structures of the Monomer and Polymer



capacity, was kept constant at $25 \pm 1^\circ\text{C}$. The feed flow rate in the flow cell was fixed at 10 L/h. After its conductivity was measured, the permeated solution was recycled to the feed tank. The salt rejection (R) describes the fraction of the depletion of salt in the permeate compared with that in the feed:

$$R(\%) = \left(1 - \frac{C_s''}{C_s'}\right) \times 100 \quad (3)$$

where C_s'' is the salt concentration in the permeate and C_s' is the salt concentration in the feed water. Both C_s'' and C_s' were measured with a standardized digital conductivity meter (model 32, YSI Co.). The calibration of the digital conductivity versus the concentration of NaCl was performed. For the minimization of experimental error, the membrane permeabilities were measured from three samples and averaged.

Mechanical strength measurements

Because of the structural characteristic of a TFC membrane, the mechanical properties of an active layer can affect the permeation properties. Therefore, it is of great interest to elucidate the effect of the mechanical strength of the active layer on the permeation performance. Measuring the mechanical properties of the active-layer films in their as-formed state is quite challenging because the films are ultrathin, and obtaining the macroscopic sizes necessary for analysis with conventional instruments such as an Instron instrument is very difficult. To this end, a promising technique, pendant drop mechanical analysis (PDMA), for di-

rectly measuring the mechanical properties of unsupported IP films was reported by Greenberg et al.¹⁸ PDMA was used to measure the mechanical resistance to rupture [rupture strength (S_R)] of thin films with a specific thickness. In PDMA, an IP active-layer film is formed at the surface of a drop of the amine solution by the drop being brought into contact with the acyl chloride solution under otherwise identical reaction conditions described in the Polymer Preparation section. After IP, the polymers were washed with pure *n*-hexane twice for the removal of unreacted monomer remnants and occluded salt and then were used for the measurement of the mechanical strength directly with no further post treatment. This film-covered drop can be pressurized in a controlled fashion, and the resulting pressure-deformation behavior can be monitored. The details of the PDMA technique, as used in this study, are discussed in an earlier article.¹⁷

Thickness measurements

For the measurement of the active-layer film thickness, the thin films were prepared on a glass plate, instead of the polysulfone support, under otherwise identical reaction conditions. The films were then washed completely and semidried in air at room temperature. The semidried films on the glass slide were sharply scratched by a shape knife, and the scratched valleys were measured with Tencor P-10 surface profilometry (Tencor Int.). The profiler tip applied 3.0 mg of force, and a scan speed of 0.1 mm/s was used for the measurements. Because the IP film possessed an irregular surface, the thickness variation was found to

be high, around 30 nm. Therefore, to for the minimization of experimental error, the thickness was measured nine times for one sample, and the average value was used.

Solubility of water and salt

The concentrations of dissolved water in the active-layer (C_w) were determined via the gravimetric method. The purified polymer was saturated with a 2000 ppm NaCl aqueous solution. The saturated polymer was retrieved from the NaCl solution, and the excess solution present in the surface of the polymer was removed with filter paper. Then, the NaCl-saturated polymer was vacuum-dried at room temperature completely. The dried and weight-measured samples were put in a chamber, which was saturated with moisture at 25°C. After 1 day, the samples were again weighed with a microbalance in the chamber, and the water solubility coefficient (C_w) was calculated as follows:

$$C_w(\text{mol}/\text{cm}^3) = \frac{|M'' - M'|/18}{V_p} \quad (4)$$

where $|M'' - M'|$ is the mass of water absorbed in the polymer (g) and V_p is the polymer volume (cm^3). For the minimization of experimental error, nine replicates were used.

To measure the salt solubility in polymers, I chose the immersion method. The dried and weighted polymer samples were immersed in a large volume (100 mL) of a 2000 ppm NaCl solution at 25°C for about 1 week. After saturation with salt, the polymer samples were retrieved from the NaCl solution, and the excess solution on the surface was removed by blotting. The blotted samples were put in a large volume (100 mL) of deionized water at 25°C and kept there for a long time to establish equilibrium. The deionized water in the beaker had previously been equilibrated with the ambient CO_2 concentration to prevent the sorption of CO_2 during the experiments. When the polymer sample was placed in the deionized water, the beaker was quickly capped, and the contents were stirred with a magnetic bar. The concentration of the desorbed salt was detected with a standardized digital conductivity meter (model 32, YSI) at 25°C. From the calibration curve, the conductivity was converted into the concentration and then the mass of salt. The solubility of salt is usually defined in terms of K_s :

$$K_s = \left(\frac{M_{SP}}{V_p} \right) / \left(\frac{M_{SS}}{V_S} \right) \quad (5)$$

where V_S is the solution volume (cm^3) and M_{SP} and M_{SS} are the salt mass in the polymer and solution (g),

TABLE II
Dispersion and Polar Force Components of Surface Tension (dyn/cm) of the Reference Liquids (20°C)

Reference liquid	γ_L^d	γ_L^p	γ_L
Water	29.1	43.7	72.8
Glycerol	37.4	26.0	63.4
Formamide	35.1	23.1	58.2

respectively. For the minimization of experimental error, nine replicates were used.

Contact-angle measurements

To study the hydrophilicity of the active thin films, we performed contact-angle measurements with an image analyzer system (PIAS, model PX-380). Sets of liquid droplets of approximately 3- μL volumes were placed on IP films and observed through a video camera. The dimensions of the liquid droplets were measured approximately 10 s after the droplets were placed on the IP film. The images of the liquid droplets were captured on videotape, and the liquid droplets were magnified before the contact angle was measured. For the minimization of experimental error, the contact angle was measured six times for each sample and then averaged. The surface tension of the dispersion and polar force for polymers can be obtained with the following equation:¹⁹

$$\cos \theta = \frac{4 \left(\frac{\gamma_s^d \gamma_L^d}{\gamma_s^d + \gamma_L^d} \right)}{\gamma_L} + \frac{4 \left(\frac{\gamma_s^p \gamma_L^p}{\gamma_s^p + \gamma_L^p} \right)}{\gamma_L} - 1 \quad (6)$$

where θ is the contact angle of the liquid and γ_L , γ_L^d , and γ_L^p are the total surface tension, dispersion force of the surface tension, and polar force of the surface tension for a standard liquid, respectively. γ_s^d and γ_s^p are the dispersion force and polar force of the surface tension for the polymer. With the contact-angle values for the reference liquids shown in Table II and the surface components of the reference liquids, the components of the surface tension for the thin-film polymers can be determined.

RESULTS AND DISCUSSION

The polyamides prepared with MPDA/TMC and PPDA/TMC have the same chemical compositions but different chemical structures. The two amine groups are in the meta position for MPDA but in the para position for PPDA. This difference in the substitution position of the amine groups produces the different monomer reactivities; the reactivity of PPDA is higher than that of MPDA.²⁰ The different reactivities and chemical structures of the monomers lead to the

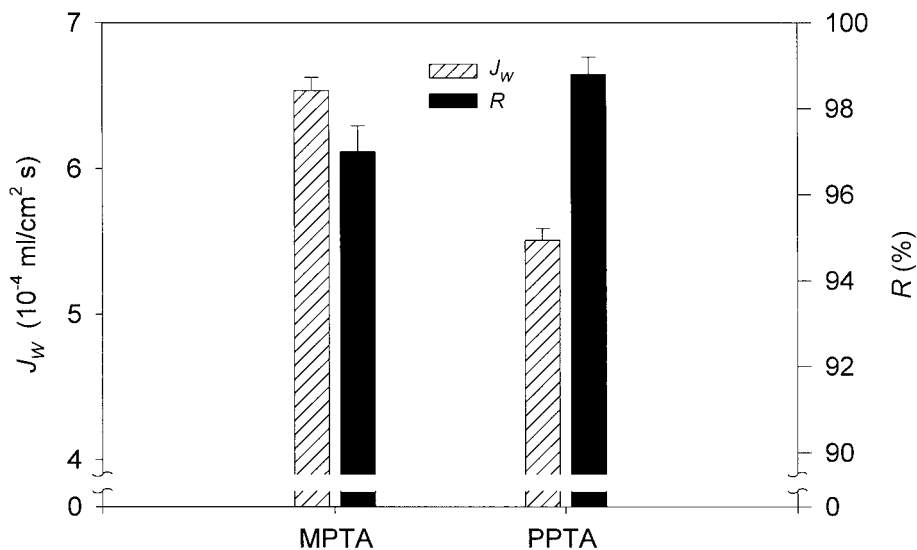


Figure 1 Effect of the aromatic amine monomer structures on the permeation performance. The membrane performance was obtained from permeation tests conducted at 3.03 MPa and 25°C with a 2000 ppm NaCl feed solution. The membranes were made with 0.5% (w/v) diamine and 0.1% (w/v) TMC.

different physicochemical properties of the polymers, including the molecular weight and free carboxylic acid content in the system (which affects the hydrophilicity).²¹

Figure 1 shows the permeation properties of the TFC membrane composed of poly(*m*-phenylene trimesamide) (MPDA/TMC or MPTA) or poly(*p*-phenylene trimesamide) (PPDA/TMC or PPTA). MPTA has a better J_w value than PPTA. The R value of PPTA, however, is higher than the MPTA. Therefore, the crosslinked aromatic polyamides with their different chemical structures show different J_w and R behaviors.

As mentioned previously, the active layer of a TFC membrane is a very thin film that bridges and overcoats the surface pores of the porous support. Because of this structural characteristic, there is the possibility that the mechanical strength of the barrier layer can affect the permeation performance of the membrane. If the thin barrier layer does not possess sufficient mechanical strength to withstand the high hydraulic pressures during the RO operation, it could partially tear, especially in the large pores at the surface of the support layer, which would lead to a bulk flow of brine and contaminate the permeated solution. S_R of the active layer is a lumped parameter that is influenced by the rupture stress (a material characteristic) and the film thickness (a structural characteristic). S_R provides an estimate of the RO conditions that will result in rupture (failure) and, therefore, defect formation in the active layer of a TFC membrane. Previous studies by Roh et al.¹⁷ and Applegate and Antonson²² have shown that the bulk flow of brine affects the permeation properties (J_w and R) of a membrane with minute defects. Using the insights provided by their study, Roh et al. determined from S_R experiments the

limiting values of S_R for water permeation (J_w) and R ; if S_R of the active layer is less than 5 kPa mm, R is affected by the bulk flow of brine. Furthermore, if S_R of the active layer is less than 3 kPa mm, both R and J_w are affected. However, if S_R is greater than 5 kPa mm, the permeation characteristics are determined only by the inherent material properties of the polyamide, including the hydrophilicity, mobility of the molecular chain, and chemical structure of the polymer. Note that this comparison of the membrane performance is based on the same experimental conditions described in a previous article.¹⁷ Therefore, the effect of the mechanical strength on the permeation performance should be examined. Figure 2 shows the S_R values of MPTA and PPTA. Both of these polyamides have S_R values greater than 5 kPa mm. This indicates that the permeation properties are the intrinsic properties of active-layer materials and, therefore, are not affected by the bulk flow of brine, which resulted in defects on the active layer because of the high hydraulic RO operation pressure.

As shown in eq. (1), J_w is inversely proportional to d , but R is independent of the thickness. Therefore, the active-layer film thicknesses were measured, and they are shown in Figure 3. The average thickness of PPTA is a little greater than that of MPTA. However, because the PPTA IP film possesses more irregular surface than the MPTA IP film and the error range is relatively broad, the thickness difference of these two IP films is not critical. This implies that the effect of the thickness of these two IP films on J_w is not prominent. That is, the different permeation properties of these two membranes are not due to the thickness of the active layer.

As described previously, the differences in the reactivities and chemical structures of the monomers yield

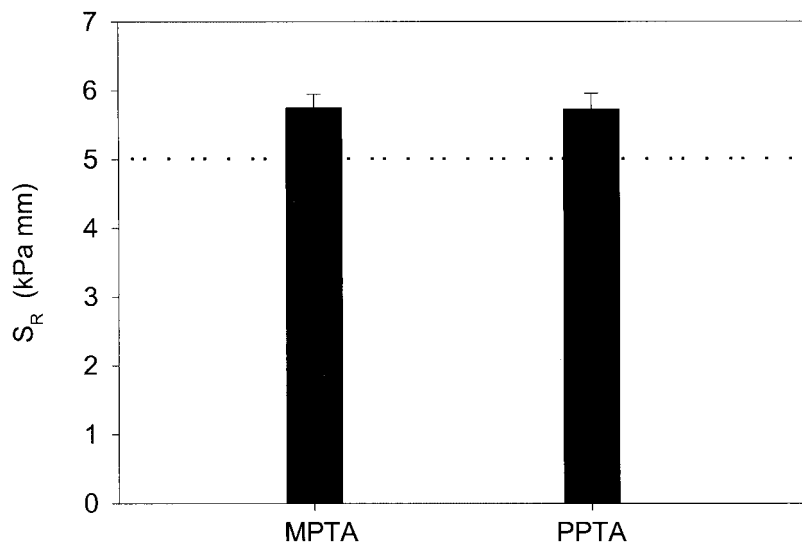


Figure 2 Dependence of S_R of the active layers on the aromatic amine structures.

different structural properties, including the degree of crosslinking and chemical properties, such as hydrophilicity.²¹ These properties affect not only the solubility but also the diffusivity of water and salt. The permeation coefficient depends on the solubility and diffusivity. Figure 4 shows the solubility of water (C_w) in the polyamides. These two polymers have different sorption properties for water. MPTA has a higher C_w value than PPTA. The absorption of water (C_w) depends on the polymer hydrophilicity. To explore the chemical properties of the active layer, we evaluated the polar force of the surface tension as a measure of the hydrophilicity of the thin active film and obtained it by conducting contact-angle measurements and using eq. (6). In these polyamides, the main components affecting the polar force are an amide bond, an amine end group, a free carboxylic acid group (an unreacted

acyl chloride group), and a carboxylic acid end group. The amine and carboxylic acid group are more hydrophilic than the amide bonds of the polyamide chain. The contents of the end groups and free carboxylic acid group are affected by the reactivity and chemical structure of the monomers. MPTA with its low reactivity has a higher polar force and better hydrophilicity. This high polar property of the polymer should result in higher water sorption than that for PPTA, as seen in Figure 4.

For the calculation of the permeation coefficient, knowledge of the solubility and diffusivity of the penetrants is necessary. Usually, the diffusivity of water or salt can be estimated via the absorption or desorption rate of the penetrants. However, because of the ultrathin thickness of the IP films (≈ 0.000015 cm), an accurate and reproducible diffusion coefficient via the

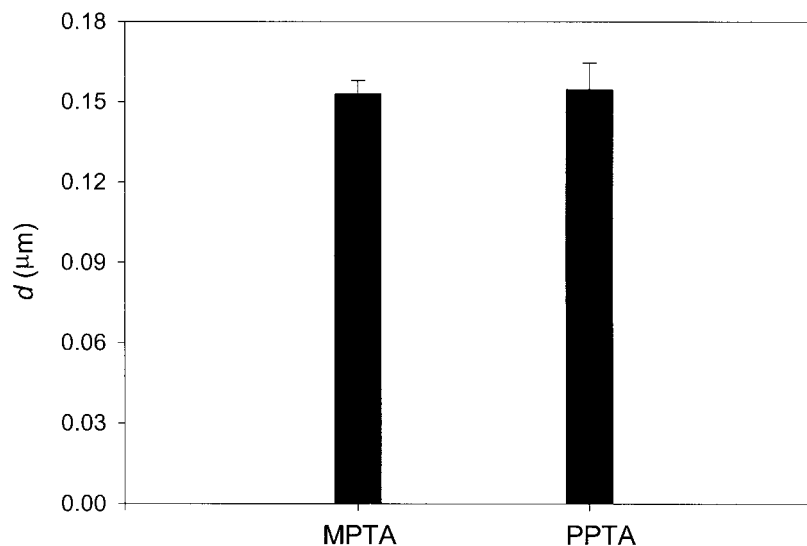


Figure 3 Dependence of d of the active layers on the aromatic amine structures.

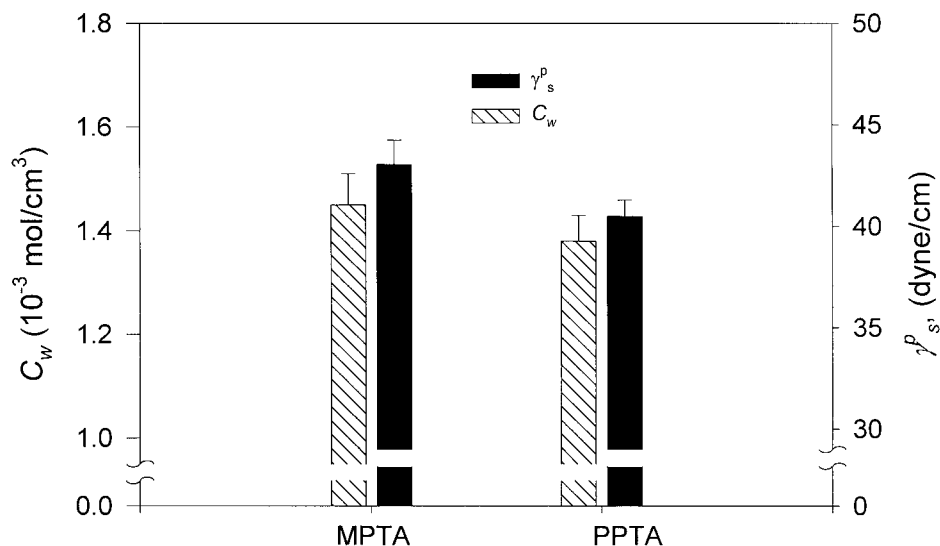


Figure 4 Dependence of γ_s^p and C_w on the aromatic amine structures.

measurement of the absorption and desorption rates was very difficult to obtain. In the absence of such information, the diffusion coefficient and permeation coefficient could not be directly calculated. Therefore, the permeation coefficient is reported in the relative form from the molecular chain mobility¹⁵ and reference data.²³

To explore the mobility of the polymer molecular chain, Kwak¹⁵ measured the spin-lattice relaxation time ($T_{1\rho}$) for the polymer chain via solid cross-polarization/magic-angle spinning ¹³C NMR, as shown in Table III. $T_{1\rho}$ is considered a useful parameter for accessing the motion of molecular chains. The molecules with larger $T_{1\rho}$ values have slower molecular motion, and low mobility, resulting in low diffusivity. The meta-positioned MPDA has a lower value of $T_{1\rho}$ than the para-positioned PPDA. The general comparative order is as follows: poly(*m*-phenylene isophthal-

amide) (MPDA/IPC or MPIA) < poly(*p*-phenylene terephthalamide) (PPDA/TPC or PPTEA), MPTA (MPDA/TMC) < PPTA (PPDA/TMC). Also, the crosslinked-structure polymers have greater values of $T_{1\rho}$ than the linear-structure polymers (MPIA < MPTA; PPTEA < PPTA). This implies that the molecular chain of MPTA is more flexible than that of PPTA, resulting in high diffusivity. Therefore, the water permeation coefficients of MPTA and PPTA can be compared, as shown in Table III. The water diffusion coefficient of MPIA, which has the lowest value of $T_{1\rho}$, is 1.5×10^{-6} cm²/s. Therefore, MPTA, having a greater $T_{1\rho}$ value than MPIA, should have a smaller D_w value than MPIA (i.e., $\ll 1.5 \times 10^{-6}$). Likewise, PPTA, having a greater value of $T_{1\rho}$ than MPTA, should have a much smaller D_w value than MPTA (i.e., $\ll 1.5 \times 10^{-6}$). Therefore, from the water solubility and relative diffusivity, the relative water permeation co-

TABLE III
Relaxation Times and Estimated Permeability Data of Water and Sodium Chloride in Aromatic Polyamides

		Polyamide			
		MPIA ^b	PPTEA ^c	MPTA ^d	PPTA ^d
Relaxation times ^a	$T_{1\rho}$ (ms)	5.34	6.29	7.94	9.17
	Checked position	C=O	C=O	C=O	C=O
Water	C_w (g/cm ³)	0.49	0.24	0.0261	0.0248
	D_w (10 ⁻⁶ cm ² /s)	1.5	<1.5	$\ll 1.5$	$\ll 1.5$
	$C_w D_w$ (10 ⁻⁷ g/cm s)	7.4	—	$\ll 0.39$	$\ll 0.37$
Salt	K_S	0.23	0.025	0.0114	0.0096
	D_S (10 ⁻¹⁰ cm ² /s)	1.5	<1.5	$\ll 1.5$	$\ll 1.5$
	$K_S D_S$ (10 ⁻¹¹ cm ² /s)	3.5	—	$\ll 0.17$	$\ll 0.14$
	$K_S D_S / C_w D_w$	—	—	≈ 0.44	≈ 0.39
	$R \approx 1 - K_S D_S / C_w D_w$	—	—	≈ 0.57	≈ 0.61

^a Ref. 15.

^b Ref. 23.

^c Ref. 26.

^d Tested and estimated.

efficient of MPTA and PPTA could be estimated (MPTA $\ll 0.039 \times 10^{-7}$ and PPTA $\ll 0.037 \times 10^{-7}$ g/cm s). This indicates that MPTA, possessing a high water permeation coefficient, has a higher J_w value than PPTA, as shown in Figure 1.

The salt permeation coefficient also can be explained in the same fashion as the water permeation coefficient. K_s values for MPTA and PPTA are shown in Table III. MPTA has a higher K_s value than PPTA. The solubility of salt in a polymer is affected by the polymer properties, including the water content²⁴ and charge density²⁵ of the polymer. In this system, the water content effect seems to be more prominent than the charge density: MPTA, having a high water content, has a higher K_s value than PPTA. As for the water diffusion behaviors, MPTA, which has a greater $T_{1\rho}$ value than PPTA, should have lower salt diffusivity than PPTA ($D_s \cong 1.5 \times 10^{-10}$ cm²/s). Moreover, PPTA, having a greater $T_{1\rho}$ value than MPTA, should have much lower salt diffusivity ($\ll 1.5 \times 10^{-10}$) than MPTA. Therefore, the salt permeation coefficient of MPTA is less than 0.017×10^{-11} cm²/s, and the coefficient of PPTA is much less than 0.014×10^{-11} cm²/s.

As previously noted in eq. (3), R describes the fraction of the depletion of salt in the permeate compared with that in the feed. Therefore, it is related to the ratio of J_s and J_w . A high R value implies that J_w is relatively high compared with J_s . Therefore, if we compare the water ($C_w D_w$) and salt permeation coefficients ($K_s D_s$) of the active layer, the differences in R can be explained. The MPTA polyamide possesses greater water and salt permeation coefficients than PPTA. However, the relative magnitude of $K_s D_s$ is much greater than that of $C_w D_w$. That is, MPTA has a higher salt-flux ratio ($K_s D_s / C_w D_w$) than PPTA (see Table III). The relatively high J_s value of MPTA leads to a low R value. This result agrees well with the R value of the TFC membrane composed of MPTA and PPTA, as shown in Figure 1.

CONCLUSIONS

Fully aromatic crosslinked polyamides synthesized with MPDA/TMC and PPDA/TMC have different permeation performances. MPTA (MPDA/TMC) shows high J_w values, but PPTA (PPDA/TMC) gives

better R values. MPTA has higher water sorption and higher molecular chain mobility than PPTA. These factors lead to higher J_w values compared with those of PPTA. However, with respect to R , PPTA has much lower salt absorption and lower molecular chain mobility than MPTA. As a result, PPTA possesses a relatively smaller salt-flux ratio ($K_s D_s / C_w D_w$) than MPTA, and this results in high R values.

References

1. Rozelle, L. T.; Cadotte, J. E.; Cobian, K. E.; Kopp, C. V., Jr. In *NS-100 Membranes for Reverse Osmosis and Synthetic Membranes*; Sourirajan, S., Ed.; National Research Council: Ottawa, Canada, 1977; p 249.
2. Cadotte, J. E. U.S. Pat. 4,277,344 (1981).
3. Eriksson, P. *J Membr Sci* 1988, 36, 297.
4. Uemura, T.; Himeshima, Y.; Kurihara, M. U.S. Pat. 4,761,234 (1988).
5. Lonsdal, H. K.; Merten, U.; Riley, R. L. *J Appl Polym Sci* 1965, 9, 1341.
6. Sherwood, T. K.; Brian, P. L. T.; Fisher, R. E. *Ind Eng Chem Fundam* 1967, 6, 2.
7. Kesting, R. E. *J Appl Polym Sci* 1990, 41, 2739.
8. Kimmerle, K.; Strathmann, H. *Desalination* 1990, 79, 283.
9. Sundet, S. A.; Arthur, S. D.; Campos, D.; Eckman, T. J.; Brown, R. G. *Desalination* 1987, 64, 33.
10. Cheng, R.; Glater, J.; Neethling, J. B.; Stenstrom, M. K. *Desalination* 1991, 85, 33.
11. Desai, N. V.; Ranggarajan, R.; Rao, A. V.; Garg, D. K.; Anleschwaria, B. V.; Mehta, M. H. *J Membr Sci* 1992, 71, 201.
12. Cadotte, J. E.; Rozelle, L. T. NTIS Report PB-229337; 1972.
13. Petersen, R. J.; Eriksson, P. K.; Cadotte, J. E. In *Frontiers of Macromolecular Science*; Saegusa, T.; Higashimura, T.; Abe, A., Eds.; Blackwell Science: London, 1989; p 511.
14. Roh, I. J.; Park, S. Y.; Kim, J.-J.; Kim, C. K. *J Polym Sci Part B: Polym Phys* 1998, 36, 1821.
15. Kwak, S.-Y. *Polymer* 1999, 40, 6361.
16. Mysels, K. J.; Wrasidlo, W. *Langmuir* 1991, 7, 3052.
17. Roh, I. J.; Kim, J.-J.; Park, S. Y. *J Membr Sci* 2002, 197, 199.
18. Greenberg, A. R.; Khare, V. P.; Krantz, W. B. *Mater Res Soc Symp Proc* 1995, 356, 541.
19. Wu, S. *J Polym Sci Part C: Polym Symp* 1971, 34, 19.
20. Ichino, T.; Sasaki, S.; Matsuura, T.; Nishi, S. *J Polym Sci Part A: Polym Chem* 1990, 28, 323.
21. Roh, I. J. *J Membr Sci* 2002, 198, 63.
22. Applegate, L. E.; Antonson, C. R. *Reverse Osmosis and Membrane Research*; Plenum: New York, 1972.
23. Frommer, M. A.; Murday, J. S.; Messalem, R. M. *Eur Polym J* 1973, 9, 367.
24. Glueckauf, E. *Desalination* 1976, 18, 155.
25. Lipp, P.; Gimbel, R.; Frimmel, F. H. *J Membr Sci* 1994, 95, 185.
26. Strathmann, H.; Michaels, A. S. *Desalination* 1977, 21, 195.